

# Gate generation for open quantum systems via a monotonic algorithm with time optimization

Paulo Sérgio PEREIRA DA SILVA<sup>‡</sup>  
 Pierre ROUCHON<sup>§</sup>

<sup>‡</sup> University of São Paulo – USP – Brazil

<sup>§</sup> Laboratoire de Physique de l'École normale supérieure,  
 Mines Paris-PSL, Inria, ENS-PSL, Université PSL, CNRS, Paris.

April 1, 2024

## Abstract

We present a monotonic numerical algorithm including time optimization for generating quantum gates for open systems. Such systems are assumed to be governed by Lindblad master equations for the density operators on a large Hilbert-space whereas the quantum gates are relative to a sub-space of small dimension. Starting from an initial seed of the control input, this algorithm consists in the repetition of the following two steps producing a new control input: (A) backwards integration of adjoint Lindblad-Master equations (in the Heisenberg-picture) from a set of final conditions encoding the quantum gate to generate; (B) forward integration of Lindblad-Master equations in closed-loop where a Lyapunov based control produced the new control input. The numerical stability is ensured by the stability of both the open-loop adjoint backward system and the forward closed-loop system. A clock-control input can be added to the usual control input. The obtained monotonic algorithm allows then to optimise not only the shape of the control input, but also the gate time. Preliminary numerical implementations indicate that this algorithm is well suited for cat-qubit gates, where Hilbert-space dimensions (2 for the Z-gate and 4 for the CNOT-gate) are much smaller than the dimension of the physical Hilbert-space involving mainly Fock-states (typically 20 or larger for a single cat-qubit). This monotonic algorithm, based on Lyapunov control techniques, is shown to have a straightforward interpretation in terms of optimal control: its stationary conditions coincides with the first-order optimality conditions for a cost depending linearly on the final values of the quantum states.

**Acknowledgment:** This project has received funding from the European Research Council (ERC) under the European Union's Horizon 2020 research and innovation programme (grant agreement No. [884762]).

## 1 Introduction

In theory, optimal control could provide fast solutions for state preparation and quantum gate generation [20, 21, 9]. The complexity of implementation of optimal control grows faster with the Hilbert dimension  $n$  [26]). This motivates the research of other methods like Lyapunov stabilization, that can tackle large dimensions [11, 18, 30, 16, 31, 22, 6, 28, 29]. Note that

Lyapunov stabilization of quantum systems appears also in the infinity-dimensional context (for instance for ensemble control of half-spin systems) [1, 15].

Several numerical algorithms have been developed for tackling quantum control. We shall call by *Piecewise-Constant* case for the algorithms that provide piecewise-constant control pulses and by *Smooth-Case* for the algorithms that provide smooth control inputs. For instance, for the Piecewise-Constant case one may consider the Krotov method [26], GRAPE (of first and second orders) [12, 5], CRAB [25], and the piecewise constant algorithm based on Lyapunov techniques [24]. For the *smooth* case, one may consider GOAT [14], and the Matlab open code available for RIGA ([23]. The Krotov method has also a *Smooth-Case* version, called here simply by *Krotov method*, that is strongly related to algorithm that is presented in this paper. The reader may refer to the survey papers [13, 10] for the description of Krotov method. One may say that the algorithm presented in this work (without clock control) is very close to the *Krotov method*, at least in the case of the so called *sequential update* of the control, which ensures a monotonic behaviour of such method<sup>1</sup>. To be monotonic in this case is a property that is analogous to the non-increasing property of the Lyapunov function in the context of the algorithm that is presented in this paper. The contributions are

- to generalise such monotonic algorithms by considering the optimisation of the shape of the control input and the gate time simultaneously (see section 5).
- to implement such generalisation on physical case-studies of bosonic qubits (see section 6) where the dimension of the underlying Hilbert-space is far much larger (578 in the numerical computations of figures 3 and 4) than the size of the orthonormal sets defining the gate (4 for a CNOT gate between two cat-qubits).

Particularly relevant for the present work is the algorithm *RIGA (Reference Input Generation Algorithm)*[23] that generates gate of small dimension  $\bar{n}$  for closed quantum systems in an Hilbert-space of larger dimension  $n \geq \bar{n}$  governed by a Schrodinger dynamics:

$$\dot{X}(t) = -\mathbf{i}(H_0 + \sum_{k=1}^m u_k H_k)X(t) \quad (1)$$

where the  $H_k$  are the Hermitian operators,  $u_k$  are scalar control inputs and  $X(t) \in U(n)$  is the propagator. The quantum gate in this case is represented by some set of initial vectors  $\{|e_i\rangle, i = 1, \dots, \bar{n}\}$  and a set of final vectors  $\{|f_i\rangle, i = 1, \dots, \bar{n}\}$ , both orthonormal subsets of  $\mathbb{C}^n$ , with  $\bar{n} \leq n$ . The gate generation relies on finding a control input  $u = (u_1, \dots, u_m)$  steering from initial value  $X(0) = I$  to a final value  $X_{goal}$  where  $X_{goal}|e_i\rangle = |f_i\rangle$ , for  $i = 1, \dots, \bar{n}$ , up to some error that is measured by the so called *gate fidelity*. This is equivalent to the following steering problem:

**Definition: 1** Let  $\{|e_i\rangle, i = 1, \dots, \bar{n}\}$  and  $\{|f_i\rangle, i = 1, \dots, \bar{n}\}$  be two orthonormal subsets of  $\mathbb{C}^n$ . The problem of quantum gate generation is to find a gate time  $T_f > 0$  and a time-varying control input  $u : [0, T_f] \rightarrow \mathbb{R}^m$  such that the solution of (1) starting form  $X(0) = I$  verifies  $X(T_f)|e_i\rangle = |f_i\rangle$  for  $i = 1, \dots, \bar{n}$  up to some admissible error called *gate-fidelity*.

---

<sup>1</sup>*Sequential update* of the control means that the control pulses that are applied to the system in a step  $\ell$  of the algorithm are updated “on the fly”, that is, not only in the end of each step as is done in the classic Krotov method and also in GRAPE.

For a prescribed gate time  $T_f$  and gate, RIGA is a monotonic algorithm improving the steering control input  $[0, T_f] \ni t \mapsto u(t)$  from an initial guess  $[0, T_f] \ni t \mapsto \bar{u}^0(t)$ . Each step  $\ell$  of RIGA is as follows. Given the control input  $\bar{u}^{\ell-1}(t)$  defined on  $[0, T_f]$ , one obtains a reference trajectory of the propagator  $X(t)$  by integrating the system backwards from the final condition  $X_{goal}$ . A Lyapunov based tracking control is then implemented, and a tracking control  $\bar{u}^\ell$  is obtained by integrating forwards the closed loop system from  $X(0) = I$ . RIGA is essentially the repetition of this process until an admissible gate fidelity is obtained. The algorithm is shown to be monotonic in the sense that the infidelity that is measured by the Lyapunov function is nonincreasing along all the steps of the algorithm. Furthermore, strong convergence results of RIGA are available for controllable closed systems [24]. Namely, for  $T_f$  big enough, RIGA converges to an exact solution of the quantum gate generation problem. Furthermore, numerical experimentations have shown that RIGA generates small control inputs with a bandwidth that contains the natural frequencies of the system, at least if the control seed  $\bar{u}^0(t)$  does not contain unnecessary high frequencies. However, it must obey some generic conditions that are fulfilled for control profile including enough harmonics of small amplitude<sup>2</sup>.

The algorithm that will be presented in this work was obtained directly from RIGA based on a Fock-Liouville representation of open quantum systems. When re-transformed back into its original representation (of a Lindblad-Master equation) this algorithm have exhibited nice physical interpretations, including the presence of the adjoint Lindblad-Master equation (in the Heisenberg picture). We have chosen to present the results directly in its final form, we shall not present here how it can be obtained from RIGA<sup>3</sup>.

So the algorithm which is the main contribution of this work can be applied for open control systems described by Lindblad Master equations on a Hilbert space of arbitrary dimension  $n$  and for a quantum gate of arbitrary dimension  $\bar{n} \leq n$ . The first part of each step  $\ell$  of this new algorithm consists in integrating backwards  $\bar{n}^2$  copies of the adjoint Lindblad equation from the final conditions  $J_\sigma(T_f), \sigma \in \Lambda$  (observables in the Heisenberg picture). The second part of the algorithm consists in integrating  $\bar{n}^2$  copies of the Lindblad Master equations with initial conditions  $\rho_\sigma(0), \sigma \in \Lambda$  in closed loop with a Lyapunov based tracking control law. The  $\bar{n}^2$  final conditions  $J_\sigma(T_f)$  and the  $\bar{n}^2$  initial conditions  $\rho_\sigma(0), \sigma \in \Lambda$  are projectors onto adequate pure states such that the quantum gate operations are ensured in an analogous way that is considered in quantum tomography context [19]. The adequate Lyapunov function for the tracking control is:

$$\mathcal{V}(t) = \bar{n}^2 - \sum_{\sigma \in \Lambda} \text{trace}(J_\sigma(t)\rho_\sigma(t))$$

It is easy to show that  $\mathcal{V}(T_f)$  corresponds to the sum of final individual gate infidelities of each member of the collection of  $\bar{n}^2$  systems. Inside each step  $\ell$ ,  $\mathcal{V}(t)$  is nonnegative, nonincreasing and  $\mathcal{V}(T_f)$  it is equal to zero if and only if  $\rho_\sigma(T_f) = J_\sigma(T_f), \sigma \in \Lambda$ , that is, the quantum gate was exactly generated. Furthermore, this algorithm is monotonic in the sense that the sequence defined by the  $\mathcal{V}(T_f)$  that are obtained along the successive steps is nonincreasing.

In this paper, we also show how to include a clock control that allows to incorporate an extra (virtual) control which may be useful for finding an “optimal” final time  $T_f$  of the gate. The clock control is in fact a virtual input  $v_0$  that controls the running of a virtual time  $\tau$  according to the differential law  $\frac{dt}{d\tau} = (1 + v_0(t))$ . Since the algorithm presented here is an

---

<sup>2</sup>See section 4.4 about the choice of the seed  $\bar{u}^0(t)$  for the proposed algorithm.

<sup>3</sup>The reader may refer to [4] for these aspects of RIGA as well as a comparison of RIGA and GRAPE.

adaptation of RIGA for open systems described by a Lindblad-Master equations, and since RIGA admits strong convergence results for the controllable unitary case, one expects that, when there exists a control  $u^*$  achieving exactly the gate and when the first variation around the trajectory associated to  $u^*$  is somehow controllable, the algorithm will converge to this set  $u^*$ , at least locally. This last conjecture will be the subject of a future research.

We also show in this paper that this algorithm may be also regarded as an iterative method that converges to a control input that satisfies the first order stationary conditions of an optimal control problem associated to the cost function  $\mathcal{V}(T_f)$ . It is also important to stress that the algorithm structure is naturally adapted for array processors that could deal with each of the  $\bar{n}^2$  copies of the system. Furthermore, the use of GPUs is strongly indicated since all the operations (including the 4-th order Runge-Kuta integration scheme) relies on the multiplication and the sum of  $n \times n$  matrices. There is no gradient computation in the process, which seems to be useful in the application on the control design of quantum systems. The numerical stability is ensured by the stability of both the adjoint system and the one of the original Lindblad equation.

Two examples of confined Cat-Qubit gates taken from [17, 8] are presented. A first example of a  $Z$ -gate, recovering the existence of an optimal final time  $T_f^*$  that was obtained in [17] with an adiabatic constant control. In this first example the fidelity of the adiabatic control is not far from the one that was produced by our algorithm, at least when both gate-times coincides to  $T_f^*$ . A second example of a CNOT-gate of much greater dimension is also studied, showing also an optimal  $T_f^*$ . However, for the second example, the shape of the control pulses are much more important. The problem of optimising the gate-time of constant adiabatic control produces an inferior fidelity (and different gate-time) than the problem of optimising both the shape and gate-time that is considered by our algorithm. The infidelity of the results of the constant adiabatic control with optimal  $T_f$  is 29.2% higher than the one of our algorithm.

The paper is organised as follows. In section 2 we state some notations and also some known results about the Lindblad master equation and its adjoint formulation. In section 3 we state the quantum gate generation problem in the context of the density operators that appear in Lindblad equations. In section 4 we present the algorithm when the gate time is prescribed and show that the algorithm is an iterative method converging to the first order stationary conditions of an optimal control problem. In section 5 we show how one can include the clock-control in this algorithm, which is useful for optimizing the final time  $T_f$  of the gate. Finally, in section 6 we shall present two worked examples for cat-qubit gates along with the results of numerical experiments with the proposed algorithm.

Throughout this work, we assume that the underlying Hilbert-spaces are of finite dimension. However as the chosen formulation uses the language of operators, the various formulas and algorithms must certainly admit a meaning in infinite dimension with suitable choices of functional spaces.

## 2 The Lindblad-Master equation

We will consider an open quantum system that is described by a Lindblad Master equation [2]. We recall that the state of a Lindblad Master equation is a  $n \times n$  density matrix  $\rho(t)$  which is a positive definite hermitian matrix of unitary trace. Let  $u = (u_1, \dots, u_m) \in \mathbb{R}^m$ ,

and let  $\rho$  be a density matrix in  $\mathbb{C}^{n \times n}$ . We may define the super-operator<sup>4</sup>

$$\mathcal{L}_u(\rho) = -\mathfrak{z} \left[ H_0 + \sum_{k=1}^m u_k H_k, \rho \right] + \sum_{q=1}^p L_q \rho L_q^\dagger - \frac{1}{2} \left\{ L_q^\dagger L_q, \rho \right\}$$

The Lindblad master equation will be denoted by:

$$\frac{d\rho(t)}{dt} = \mathcal{L}_{u(t)}(\rho(t))$$

We shall also consider the adjoint Lindblad-Master equation. The state  $J(t)$  of the adjoint Lindblad Master equation, called *Observable*, is a  $n \times n$  hermitian matrix  $J(t)$ . In our algorithm, such observable  $J(t)$ , will be such that its spectrum is always contained in  $[0, 1]$ . The adjoint Lindblad equation given below considers in fact the Heisenberg view-point of quantum mechanics with the super-operator

$$\mathcal{L}_u^*(J) = -\mathfrak{z} \left[ -H_0 - \sum_{k=1}^m u_k H_k, J \right] + \sum_{q=1}^p L_q^\dagger J L_q - \frac{1}{2} \left\{ L_q^\dagger L_q, J \right\} \quad (2)$$

defining the adjoint Lindblad equation [2]:

$$\frac{dJ(t)}{dt} = \mathcal{L}_{u(t)}^*(J(t))$$

It is well known that, if one takes an observable  $J(0)$  and compute the solution of the Lindblad-Master equation  $\rho(t)$ , and after that one computes the expectation value of the observable, this entire process is equivalent to take the initial condition of the state and compute the expectation value of the observable  $J(t)$ . In other words:

$$\text{trace}(J(0)\rho(t)) = \text{trace}(J(t)\rho(0)) \quad (3)$$

The condition (3) will be important in order to ensure that our algorithm is monotonic.

### 3 Quantum gate generation problem

As said in the introduction, for closed quantum system and considering the unitary evolution of the Schrodinger equation (1), the quantum gate generation problem can be stated as being the steering problem of Def. 1. For open quantum systems, in the case where the state is a density operator, the quantum gate generation problem may be defined in a way that is similar to the quantum Tomography context [19]. This consists in constructing a set of pure states assuring the complete definition of the gate.

**Definition: 2** (*Quantum Gate Generation Problem*) Consider that  $\{|e_i\rangle, i = 1, \dots, \bar{n}\}$  and  $\{|f_i\rangle, i = 1, \dots, \bar{n}\}$  are two orthonormal subsets of  $\mathbb{C}^n$  with  $\bar{n} \leq n$ . Let

- $|e_{ijR}\rangle = \frac{1}{\sqrt{2}}(|e_i\rangle + |e_j\rangle)$ ,  $i > j$ , and  $|e_{ijI}\rangle = \frac{1}{\sqrt{2}}(|e_i\rangle + \mathfrak{z}|e_j\rangle)$ ,  $i > j$
- $|f_{ijR}\rangle = \frac{1}{\sqrt{2}}(|f_i\rangle + |f_j\rangle)$ ,  $i > j$ , and  $|f_{ijI}\rangle = \frac{1}{\sqrt{2}}(|f_i\rangle + \mathfrak{z}|f_j\rangle)$ ,  $i > j$ .

---

<sup>4</sup>To avoid notation confusion in the sequel with indice  $i$  we use the bold symbol  $\mathfrak{z}$  for  $\sqrt{-1}$ .

The quantum gate generation problem consists in finding a set of  $m$  control pulses  $u : [0, T_f] \rightarrow \mathbb{R}^m$  such that:

(i) The state  $\rho(t)$  is steered from the state  $|e_i\rangle\langle e_i|$  at  $t = 0$  to the state  $|f_i\rangle\langle f_i|$ , at  $t = T_f$  for  $i = 1, \dots, \bar{n}$

(ii) One must also steer all the  $|e_{ijR}\rangle\langle e_{ijR}|$  at  $t = 0$  to  $|f_{ijR}\rangle\langle f_{ijR}|$  at  $t = T_f$ .

(iii) One must also steer all the  $|e_{ijI}\rangle\langle e_{ijI}|$  at  $t = 0$  to  $|f_{ijI}\rangle\langle f_{ijI}|$  at  $t = T_f$ .

We stress that all the final and initial conditions that defines the gate are pure states. We shall consider a set of  $\bar{n}^2$  multi-indices  $\sigma$  elements of

$$\Lambda = \{i, ijR, ijI : i, j \in \{1, \dots, \bar{n}\}, i > j\}.$$

for indexing the above family of initial and final conditions.

## 4 Monotonic algorithm with a prescribed gate-time

This section is devoted to the description of the proposed algorithm.

### 4.1 Main definitions

Decompose the control input  $u$  as  $u(t) = \bar{u}(t) + \tilde{u}(t)$  where  $\bar{u}(t)$  appears in  $\bar{n}^2$  copies of the (minus) adjoint Lindblad Master equation with different final conditions indexed by  $\sigma \in \Lambda$ :

$$\frac{dJ_\sigma}{dt}(t) = -\mathcal{L}_{\bar{u}(t)}^*(J_\sigma(t)) \quad (4a)$$

$$J_\sigma(T_f) = \Pi_{|\phi_\sigma\rangle} = |\phi_\sigma\rangle\langle\phi_\sigma|, \sigma \in \Lambda \quad (4b)$$

where

$$|\phi_\sigma\rangle = \begin{cases} |f_i\rangle, & \text{if } \sigma = i \in \{1, \dots, \bar{n}\} \\ \frac{|f_i\rangle + |f_j\rangle}{\sqrt{2}}, & \text{if } \sigma = ijR, i, j \in \{1, \dots, \bar{n}\}, i > j \\ \frac{|f_i\rangle + \mathbf{u}|f_j\rangle}{\sqrt{2}}, & \text{if } \sigma = ijI, i, j \in \{1, \dots, \bar{n}\}, i > j \end{cases}$$

Then  $u = \bar{u} + \tilde{u}$  appears in  $\bar{n}^2$  copies of the system with different initial conditions:

$$\frac{d\rho_\sigma(t)}{dt} = \mathcal{L}_{\bar{u}(t) + \tilde{u}(t)}(\rho_\sigma(t)) \quad (5a)$$

$$\rho_\sigma(0) = \Pi_{|\epsilon_\sigma\rangle} = |\epsilon_\sigma\rangle\langle\epsilon_\sigma|, \sigma \in \Lambda \quad (5b)$$

where

$$|\epsilon_\sigma\rangle = \begin{cases} |e_i\rangle, & \text{if } \sigma = i \in \{1, \dots, \bar{n}\} \\ \frac{|e_i\rangle + |e_j\rangle}{\sqrt{2}}, & \text{if } \sigma = ijR, i, j \in \{1, \dots, \bar{n}\}, i > j \\ \frac{|e_i\rangle + \mathbf{u}|e_j\rangle}{\sqrt{2}}, & \text{if } \sigma = ijI, i, j \in \{1, \dots, \bar{n}\}, i > j \end{cases}$$

## 4.2 The Lyapunov Function

We shall apply a Lyapunov based feedback law in the input  $\tilde{u}$  to be described in the sequel. For this, consider the Lyapunov function:

$$\mathcal{V}(t) = \bar{n}^2 - \sum_{\sigma \in \Lambda} \text{trace}(J_\sigma(t)\rho_\sigma(t))$$

where  $J_\sigma(t)$  and  $\rho_\sigma(t)$  are solution of (4) and (5), respectively. It is clear  $\mathcal{V}(T_f)$  is the sum of the gate-infidelities of the members of the system for all  $\sigma \in \Sigma$  since

$$\text{trace}(\Pi_{|\phi_\sigma\rangle}\rho) = \text{trace}(|\phi_\sigma\rangle\langle\phi_\sigma|\rho) = \langle\phi_\sigma|\rho|\phi_\sigma\rangle$$

which is the fidelity of  $\rho$  with respect to the pure state  $|\phi_\sigma\rangle$ .

The following proposition explains why  $\mathcal{V}(t)$  is a convenient Lyapunov function for the quantum gate generation problem.

**Proposition: 1** *Take  $\sigma \in \Lambda$  and  $(J_\sigma, \rho_\sigma)$  solutions of (4,5). Then necessarily for any  $t \in [0, T_f]$ ,  $0 \leq \text{trace}(J_\sigma(t)\rho_\sigma(t)) \leq 1$ . Thus  $\mathcal{V}(t) \geq 0$ . Moreover if  $\mathcal{V}(T_f) = 0$  then for all  $\sigma \in \Lambda$ ,  $\rho_\sigma(T_f) = |\phi_\sigma\rangle$ .*

The proof of this proposition just relies on the fact that for all  $t \in [0, T_f]$ , the spectrum of  $J_\sigma(t)$  belongs to  $[0, 1]$  according to [27] and that  $\rho_\sigma(t)$  is a density operator.

Computing the time-derivative of the Lyapunov function, one gets:

$$\begin{aligned} \frac{d\mathcal{V}(t)}{dt} &= - \sum_{\sigma \in \Lambda} \text{trace} \left( \frac{dJ_\sigma}{dt}(t)\rho_\sigma(t) + J_\sigma(t)\frac{d\rho_\sigma(t)}{dt} \right) \\ &= - \sum_{\sigma \in \Lambda} \text{trace}(-\mathcal{L}_{\bar{u}}^*(J_\sigma(t))\rho_\sigma(t)) + \text{trace}(J_\sigma(t)\mathcal{L}_{(\bar{u}+\tilde{u})}(\rho_\sigma(t))) \\ &= - \sum_{k=1}^m \tilde{u}_k \left[ \sum_{\sigma \in \Lambda} \text{trace}(J_\sigma(t)[-iH_k, \rho_\sigma(t)]) \right] \end{aligned}$$

In the computations above we have used the fact that  $\mathcal{L}_u(\rho)$  is affine in  $u$  and

$$\text{trace}(-\mathcal{L}_{\bar{u}}^*(J_\sigma)\rho_\sigma) + \text{trace}(J_\sigma\mathcal{L}_{\bar{u}}(\rho_\sigma)) = 0.$$

Assume that  $[0, T_f] \ni t \mapsto \bar{u}(t)$  is given, then the Lyapunov-based control with strictly positive gain  $g_k > 0$  provides  $\tilde{u}$  via the forward integration of (5):

$$u_k(t) = \bar{u}_k(t) + g_k \underbrace{\left[ \sum_{\sigma \in \Lambda} \text{trace}(J_\sigma(t)[-iH_k, \rho_\sigma(t)]) \right]}_{\tilde{u}_k = g_k F_k(t)}$$

By construction :

$$\frac{d\mathcal{V}(t)}{dt} = - \sum_{k=1}^m g_k F_k^2(t) \leq 0$$

and so the Lyapunov function is nonincreasing inside a specific step  $\ell$  of the algorithm.

### 4.3 The algorithm

We are ready to state the main contribution of this paper which is the following algorithm.

#### BEGIN ALGORITHM

‡1. Choose the seed input  $\bar{u}^0 : [0, T_f] \rightarrow \mathbb{R}^m$ .

**BEGIN STEP  $\ell$ .**

‡2. Set  $\bar{u}(\cdot) = \bar{u}^{\ell-1}(\cdot)$ .

Integrate (backwards) in  $[0, T_f]$  the  $\bar{n}^2$  copies of the adjoint system:

$$\frac{dJ_\sigma}{dt}(t) = -\mathcal{L}_{\bar{u}(t)}^*(J_\sigma(t)), \quad J_\sigma(T_f) = \Pi_{|\phi_\sigma\rangle} = |\phi_\sigma\rangle\langle\phi_\sigma|, \sigma \in \Lambda$$

‡3. Integrate (forward) in  $[0, T_f]$  the  $\bar{n}^2$  copies of the system in closed loop:

$$\begin{aligned} \frac{d\rho_\sigma(t)}{dt} &= \mathcal{L}_{u(t)}(\rho_\sigma(t)), \quad \rho_\sigma(0) = \Pi_{|\epsilon_\sigma\rangle}, \sigma \in \Lambda \\ u_k(t) &= \bar{u}_k(t) + \underbrace{\sum_{\sigma \in \Lambda} \text{trace}(J_\sigma(t)[-iH_k, \rho_\sigma(t)])}_{\tilde{u}_k(t) = g_k F_k(t), g_k > 0}, k = 1, \dots, m \end{aligned}$$

Set  $\bar{u}^\ell(\cdot) = u(\cdot)$  (closed loop input).

Notice that control constraints can be included here just by imposing that each  $u_k(t)$  remains between  $u_k^{\min}$  and  $u_k^{\max}$ .

‡4. If the final fidelity is acceptable, then terminate the algorithm. Otherwise, execute step  $\ell + 1$ .

**END STEP  $\ell$**

#### END ALGORITHM

**Theorem: 1** *The value of the Lyapunov function  $\mathcal{V}(T_f)$  obtained in the end of the step  $\ell - 1$  of the previous algorithm is equal to the initial value  $\mathcal{V}(0)$  for step  $\ell + 1$ . In particular the Lyapunov function is non-increasing along all the steps of the algorithm.*

**Proof:** In ‡3. of step  $\ell$  we integrate (forward):

$$\begin{aligned} \frac{d\rho_\sigma(t)}{dt} &= \mathcal{L}_{u(t)}(\rho_\sigma(t)), \quad \rho_\sigma(0) = \Pi_{|\epsilon_\sigma\rangle}, \sigma \in \Lambda \\ u(t) &= \bar{u}^\ell(t) \end{aligned}$$

We stress that all the initial condition are the same  $\rho_\sigma(0), \sigma \in \Lambda$  for all  $\ell = 1, 2, \dots$ . Now note that, in ‡2. of step  $\ell + 1$ , we integrate backwards

$$\begin{aligned} \frac{dJ_\sigma}{dt}(t) &= -\mathcal{L}_{\bar{u}(t)}^*(J_\sigma(t)), \quad J_\sigma(T_f) = \Pi_{|\phi_\sigma\rangle} = |\phi_\sigma\rangle\langle\phi_\sigma|, \sigma \in \Lambda \\ \bar{u}(t) &= \bar{u}^\ell(t) \end{aligned}$$



Note that, as we integrate backwards  $-\mathcal{L}_{\bar{u}(t)}^*$ , that is, the time reversing of the adjoint system, then  $J_\sigma(0)$  plays the role of the final observable, whereas  $J_\sigma(T_f)$  plays the role of the initial observable. Then the Schrodinger/Heisenberg duality gives:

$$\underbrace{\text{trace}(J_\sigma(0)\rho_\sigma(0))}_{\text{defines } \mathcal{V}(0) \text{ for step } \ell + 1} = \underbrace{\text{trace}(J_\sigma(T_f)\rho_\sigma(T_f))}_{\text{defines } \mathcal{V}(T_f) \text{ for step } \ell}$$

□

#### 4.4 Choice of the seed

We state now some remarks about the choice of the seed  $\bar{u}^0(t)$  of the proposed algorithm. We may choose an integer  $M > 0$ , a period  $T > 0$  and small amplitude  $\mathbf{A} > 0$  and two vectors  $\mathbf{a}$ ,  $\mathbf{b}$  in  $\mathbb{R}^{m \times M}$  with **random**, independent, and uniformly distributed entries in  $[-1, 1]$ :

$$\begin{aligned} \mathbf{a} &= \{a_{k,\ell}, k = 1, \dots, m, \ell = 1, \dots, M\} \\ \mathbf{b} &= \{b_{k,\ell}, k = 1, \dots, m, \ell = 1, \dots, M\} \end{aligned}$$

So define the seed  $\bar{u}^0$  from a given reasonable initial control  $[0, T_f] \ni t \mapsto u^{init}(t)$  perturbed as follows:

$$\bar{u}_k^0(t) = u_k^{init}(t) + \mathbf{A} \left\{ \sum_{\ell=1}^M [a_{k\ell} \sin(2\ell\pi t/T) + b_{k\ell} \cos(2\ell\pi t/T)] \right\} \quad (6)$$

Such choices are inspired from a mathematical result given in [24] for purely controllable Hamiltonian dynamics and requiring that the seed must contain the presence of sufficient harmonics in order to guarantee the convergence to an exact gate generation. For  $M$  big enough, this convergence is ensured with probability one with respect to the random variables  $\mathbf{a}$ ,  $\mathbf{b}$ . This is due to the fact that the proof is based on the main ideas of the Coron's return method [3].

#### 4.5 Optimal control interpretation

In this section we shall show that our algorithm converges to a control law that obeys the stationary conditions of first order of an optimal control problem. We consider the notations used in (4,5) for the quantum states  $\Pi_{|\epsilon_\sigma\rangle}$  and observables  $\Pi_{|\phi_\sigma\rangle}$ ,  $\sigma \in \Lambda$  defining a quantum gate. We will consider the same set of  $\bar{n}^2$  copies of the system:

$$\frac{d\rho_\sigma(t)}{dt} = \mathcal{L}_u(\rho_\sigma(t)) = \mathcal{L}_0(\rho_\sigma(t)) + \sum_{k=1}^m u_k [-\mathbf{v}H_k, \rho_\sigma(t)], \quad \rho_\sigma(0) = \Pi_{|\epsilon_\sigma\rangle}, \sigma \in \Lambda \quad (7)$$

Consider the following optimal control problem:

$$\begin{aligned} \text{Find } u : [0, T_f] \rightarrow \mathbb{R}^m \text{ in order to minimise: } & \bar{n}^2 - \sum_{\sigma \in \Lambda} \text{trace}(\Pi_{|\phi_\sigma\rangle} \rho_\sigma(T_f)) \text{ subject to} \\ & \frac{d\rho_\sigma(t)}{dt} = \mathcal{L}_u(\rho_\sigma(t)), \quad \rho_\sigma(0) = \Pi_{|\epsilon_\sigma\rangle}, \sigma \in \Lambda. \end{aligned}$$

Consider the Lagrangian

$$\bar{n}^2 - \sum_{\sigma \in \Lambda} \text{trace}(\Pi_{|\phi_\sigma\rangle} \rho_\sigma(T_f)) + \sum_{\sigma \in \Lambda} \int_0^{T_f} \text{trace} \left( J_\sigma(t) (\mathcal{L}_u(t) - \frac{d\rho_\sigma(t)}{dt}) \right) dt$$

with the adjoint operators  $J_\sigma(t)$ . The stationary conditions of this Lagrangian versus any variation  $\delta\rho_\sigma(t)$  such that  $\delta\rho_\sigma(0) = 0$  yield to the adjoint system for  $J_\sigma$  with its final conditions:

$$\forall\sigma \in \Lambda, \forall t \in [0, T_f], \frac{dJ_\sigma}{dt}(t) = -\mathcal{L}_{u(t)}^*(J_\sigma(t)), \quad J_\sigma(T_f) = \Pi_{|\phi_\sigma\rangle} = |\phi_\sigma\rangle\langle\phi_\sigma| \quad (8)$$

The stationary conditions of this Lagrangian versus any variation  $\delta u(t)$  yield to

$$\forall t \in [0, T_f], \forall k \in \{1, \dots, m\}, F_k(t) = \sum_{\sigma \in \Lambda} \text{trace}(J_\sigma(t)[-iH_k, \rho_\sigma(t)]) = 0, \quad (9)$$

Equations (7), (8) and (9) are thus the first order stationary conditions of the above optimal control problem.

Returning to our algorithm, recall that:

- The sequence  $\mathcal{V}_\ell = \mathcal{V}(T_f)$  is nonnegative and nondecreasing along the steps  $\ell = 1, 2, \dots$  of the algorithm. Hence, this sequence must converge to some  $\mathcal{V}^* \geq 0$ .
- Recall that  $\frac{d\mathcal{V}}{dt} = -\sum_{k=1}^m g_k F_k^2(t)$  with  $\tilde{u}_k(t) = g_k F_k(t)$ .
- Then  $\underbrace{\mathcal{V}_{\ell-1}}_{\mathcal{V}(0)} - \underbrace{\mathcal{V}_\ell}_{\mathcal{V}(T_f)} = \sum_{k=1}^m \int_0^{T_f} g_k F_k^2(t) dt \rightarrow 0$  in the compact interval  $[0, T_f]$ .
- It is easy to show that  $\frac{dF_k}{dt}$  is bounded (because  $\frac{d\rho_\sigma}{dt}$  and  $\frac{dJ_\sigma}{dt}$  are bounded) and so the  $F_k, F_k^2$  are bounded and Lipchitz continuous.
- In particular,  $F_k(t) \rightarrow 0$  in the sup norm for all  $k = 1, \dots, m$  when the iteration step  $\ell$  tends to infinity. This results from the monotonicity of the algorithm.

Thus the monotonic algorithm converges to some  $u$  satisfying the first order stationary conditions (7), (8) and (9), which is equivalent to say that the feedback  $\tilde{u}$  converges to zero as the iteration number  $\ell$  goes to the infinity.

## 5 Monotonic algorithm with gate-time optimization

The idea of ‘‘controlling the clock’’ appears for instance in [7] in the context of ‘‘orbital flatness’’ (see the references therein for a control historical perspective). By controlling the clock we mean that we can introduce a virtual time  $\tau$  such that  $\frac{dt}{d\tau} = (1 + v_0(\tau))$  where  $v_0$  is the control of the clock. Basically the virtual time  $\tau$  can run faster ( $v_0 < 0$ ) or slower ( $v_0 > 0$ ) than the real time  $t$ . This procedure ensures the existence of a new (virtual) control  $v_0$  for the system. By controlling the clock one also changes the final time  $T_f$  that is associated to the control problem. Denote:

$$\begin{aligned} \mathcal{L}_0(\rho) &= -i[H_0, \rho] + \sum_{q=1}^p L_q \rho L_q^\dagger - \frac{1}{2} \left\{ L_q^\dagger L_q, \rho \right\} \\ \mathcal{L}_k(\rho) &= -i[H_k, \rho], \quad k = 1, \dots, m \end{aligned}$$

Then the Lindblad master equation reads:

$$\frac{d\rho}{dt} = \mathcal{L}_0(\rho) + \sum_{k=1}^m u_k(t) \mathcal{L}_k(\rho)$$

The virtual time  $\tau$  produced by a clock-control  $v_0(\tau)$  via

$$\frac{dt}{d\tau} = (1 + v_0(\tau)) = \alpha(\tau).$$

cannot reverse the time direction. Thus we include the restriction  $|v_0(\tau)| < 1$ . Note that the real time  $t(\tau)$  is given by  $t(\bar{\tau}) = \int_0^{\bar{\tau}} \alpha(\tau) d\tau$ . Then, defining  $v_k(\tau) = (1 + v_0(\tau))u_k[t(\tau)]$  for  $k \in \{1, \dots, m\}$ , one obtains:

$$\begin{aligned} \frac{d\rho}{d\tau} &= \frac{d\rho}{dt} \frac{dt}{d\tau} = (1 + v_0(\tau))(\mathcal{L}_0(\rho) + \sum_{k=1}^m u_k \mathcal{L}_k(\rho)) \\ &= \left( \mathcal{L}_0(\rho) + \sum_{k=0}^m v_k(\tau) \mathcal{L}_k(\rho) \right) \end{aligned}$$

with  $m + 1$  virtual scalar control inputs

$$v(\tau) = (v_0(\tau), v_1(\tau), \dots, v_m(\tau)) \in \mathbb{R}^{m+1}.$$

Denote:

$$\mathcal{L}_0^*(\rho) = \mathfrak{L}[H_0, \rho] + \sum_{q=1}^p L_q^\dagger \rho L_q - \frac{1}{2} \left\{ L_q^\dagger L_q, \rho \right\}$$

And define the adjoint superoperator

$$\mathcal{L}_k^*(\rho) = \mathfrak{L}[H_k, \rho], k = 1, \dots, m$$

Then, given the system with clock control:

$$\frac{d\rho}{d\tau} = \mathcal{L}_0(\rho) + \sum_{k=0}^m v_k(\tau) \mathcal{L}_k(\rho)$$

Its corresponding adjoint system is given by:

$$\frac{dJ}{d\tau} = \mathcal{L}_0^*(J) + \sum_{k=0}^m v_k(\tau) \mathcal{L}_k^*(J)$$

Then we may state the algorithm equipped with clock control

### BEGIN ALGORITHM

[#0.] Choose  $T_f^{(0)}$  and the **seed input**  $\bar{u}^0 : [0, T_f^{(0)}] \rightarrow \mathbb{R}^m$ .

### BEGIN STEP $\ell$ .

- #1. Let  $T_f = T_f^{(\ell-1)}$ . Define  $\bar{v} : [0, T_f] \rightarrow \mathbb{R}^{m+1}$ , with  $\bar{v}_0(\tau) = 0$  and  $\bar{v}_k(\tau) = \bar{u}_k^{\ell-1}(\tau), \forall \tau \in [0, T_f], k = 1, \dots, m$ .
- #2. Set  $\bar{v}(\tau) = \bar{v}^{\ell-1}(\tau)$ . Integrate (backwards) the  $\bar{n}^2$  copies of the adjoint system in  $[0, T_f]$ . Obtain the trajectories  $J_\sigma(\tau)$ , for  $\tau \in [0, T_f]$  with final condition  $J_\sigma(T_f) = \Pi_{|\phi_\sigma}$ ,  $\sigma \in \Lambda$ .

- #3. Integrate the  $\bar{n}^2$  copies of the closed loop system in  $[0, T_f]$ .  
 Obtain the trajectories  $\rho_\sigma(\tau)$ , for  $\tau \in [0, T_f]$  with initial condition  $\rho_\sigma(0) = \Pi_{|\epsilon_\sigma\rangle}$ .  
 Set  $\bar{v}_k^\ell(\tau) = \bar{v}_k(\tau) + g_k \sum_{\sigma \in \Lambda} \text{trace}(J_\sigma(\tau) \mathcal{L}_k(\rho_\sigma(\tau)))$ ,  $k = 0, 1, \dots, m$  and gains  $g_k > 0$ .
- #4. Compute the new final time  $T_f^{(\ell)} = \int_0^{T_f} (1 + \bar{v}_0^\ell(\tau)) d\tau$ .  
 Compute  $\bar{u}_k^\ell(t(\tau)) = \frac{\bar{v}_k^\ell(\tau)}{1 + \bar{v}_0^\ell(\tau)}$ , for  $\tau \in [0, T_f]$ ,  $k=1, \dots, m$   
 where  $t(\tau) = \int_0^\tau (1 + v_0(\tau')) d\tau'$ .
- #5. If the final fidelity is acceptable, then terminate. Otherwise, execute step  $\ell + 1$ .

**END STEP  $\ell$ .**

**END ALGORITHM.**

The corresponding optimal control problem is then

$$\begin{aligned} \text{Find } T_f > 0 \text{ and } u : [0, T_f] \rightarrow \mathbb{R}^m \text{ in order to minimise: } \bar{n}^2 - \sum_{\sigma \in \Lambda} \text{trace}(\Pi_{|\phi_\sigma\rangle} \rho_\sigma(T_f)) \\ \text{subject to } \frac{d\rho_\sigma(t)}{dt} = \mathcal{L}_u(\rho_\sigma(t)), \rho_\sigma(0) = \Pi_{|\epsilon_\sigma\rangle}, \sigma \in \Lambda. \end{aligned}$$

The first order stationary conditions (7), (8) and (9) have to be completed by the following condition relative to the variation of  $T_f$ :

$$\sum_{\sigma \in \Lambda} \text{trace}(\Pi_{|\phi_\sigma\rangle} \mathcal{L}_u(\rho_\sigma(T_f))) = 0. \quad (10)$$

It is then clear that the above monotonic algorithm including clock-control always converges to some  $u$  and  $T_f > 0$  satisfying these first order stationary conditions.

## 6 Numerical simulations for confined cat-qubit gates

The next two gate generations are taken from [17, 8] combining dissipative dynamics towards the code space with adiabatic Hamiltonian dynamics for cat-qubit gates.

### 6.1 Z-gate

Define the dissipation super operator:

$$\mathcal{D}[L]\rho = L\rho L^\dagger - \frac{1}{2}\{L^\dagger L, \rho\}.$$

Following [17, equation (5)] consider the following Lindblad equation

$$\frac{d\rho(t)}{dt} = \kappa_2 \mathcal{D}[a^2 - \alpha^2]\rho + \kappa_1 \mathcal{D}[a]\rho - \mathbf{u}[H_c, \rho]$$

where  $a$  is the annihilation operator of an harmonic quantum oscillator with infinite dimensional Hilbert space with Fock Hilbert basis  $\left(|n\rangle\right)_{n \geq 0}$ :  $a|n\rangle = \sqrt{n}|n-1\rangle$ ;  $\alpha$  is any real number ( $\alpha^2 \equiv \alpha^2 I$  with  $I$  identity operator), and the control Hamiltonian associated to the scalar control  $u$  is given by  $H_c = (a + a^\dagger)$ .

We have chosen  $\kappa_2 = 1$  and  $\kappa_1 = 1/100$ . We have taken  $\alpha = 2$  and we have truncated the Hilbert basis up to  $n^{\max} = 20$  Fock states (including  $|0\rangle$ ). The definition of coherent state  $|\alpha\rangle$  reads:

$$|+\alpha\rangle = \exp\left(\frac{-|\alpha|^2}{2}\right) \sum_{n=0}^{\infty} \frac{\alpha^n}{\sqrt{n!}} |n\rangle$$

We define respectively the even and odd parity cats of norm one:

$$|C_{\alpha}^{\pm}\rangle \propto |+\alpha\rangle \pm |-\alpha\rangle$$

From a unitary evolution point of view, our quantum gate may be defined as the following steering problem: steer  $|C_{\alpha}^+\rangle$  to  $|C_{\alpha}^-\rangle$ , and steer  $|C_{\alpha}^-\rangle$  to  $|C_{\alpha}^+\rangle$ .<sup>5</sup>

Define:  $|e_{12R}\rangle = \frac{|e_1\rangle+|e_2\rangle}{\sqrt{2}}$ ,  $|e_{12I}\rangle = \frac{|e_1\rangle+i|e_2\rangle}{\sqrt{2}}$ ,  $|f_{12R}\rangle = \frac{|f_1\rangle+|f_2\rangle}{\sqrt{2}}$ ,  $|f_{12I}\rangle = \frac{|f_1\rangle+i|f_2\rangle}{\sqrt{2}}$ . As in Definition 2, the operations defining the Z-gate in the context of density matrices are: steer  $|e_1\rangle\langle e_1|$  to  $|f_1\rangle\langle f_1|$  at  $t = T_f$ , steer  $|e_2\rangle\langle e_2|$  to  $|f_2\rangle\langle f_2|$  at  $t = T_f$ , steer  $|e_{12R}\rangle\langle e_{12R}|$  to  $|f_{12R}\rangle\langle f_{12R}|$  at  $t = T_f$  and steer  $|e_{12I}\rangle\langle e_{12I}|$  to  $|f_{12I}\rangle\langle f_{12I}|$  at  $t = T_f$ .

For realising this gate at  $t = T_f$ , we have a well known nice constant (turning) adiabatic control:

$$[0, T_f] \ni t \mapsto u(t) = u_{ad} \equiv \frac{\pi}{4T_f\alpha} \quad (11)$$

ensuring, when  $\kappa_1 = 0$ , an almost perfect gate for  $T_f$  large enough. When  $\kappa_1 > 0$ ,  $T_f$  cannot be chosen too large (typically  $T_f\kappa_1 \ll 1$ ) in order to avoid the decoherence due to photon losses at rate  $\kappa_1$ . In all simulations, the seed input  $\bar{u}^0(t)$  is considered to be the adiabatic control slightly perturbed by the sum of harmonics

$$\bar{u}^0(t) = u_{ad}(t) + \mathbf{A} \sum_{\ell=1}^M [a_{k\ell} \sin(2\ell\pi t/T) + b_{k\ell} \cos(2\ell\pi t/T)], \quad (12)$$

with  $T = T_f^{(0)}$ , and  $\mathbf{A} = \frac{|u_{ad}|}{100}$ ,  $M = 3$ . The control gain is  $g_1 = 1$ ,  $k = 1, \dots, m$ . The gain of the clock-control is  $g_0 = 0.1$ .

Given a pure state  $\Pi_{|\xi\rangle} = |\xi\rangle\langle\xi|$  with  $|\xi\rangle \in \mathbb{C}^n$  and a density matrix  $\rho$ , the fidelity function is:

$$\text{Fidelity}(\rho, \Pi_{|\xi\rangle}) = \langle\xi| \rho |\xi\rangle$$

Recall that the final conditions defining the quantum gate are given by pure states:

$$J_{\sigma}(T_f) = \Pi_{|\phi_{\sigma}\rangle} = |\phi_{\sigma}\rangle\langle\phi_{\sigma}|, \sigma \in \Lambda.$$

The gate infidelity  $\mathcal{I}$  in the end of each step of the algorithm will be defined by

$$\mathcal{I} = \max_{\sigma \in \Lambda} \{1 - \text{Fidelity}(\rho_{\sigma}(T_f), |\phi_{\sigma}\rangle\langle\phi_{\sigma}|)\} = \max_{\sigma \in \Lambda} \{1 - \langle\phi_{\sigma}| \rho_{\sigma}(T_f) |\phi_{\sigma}\rangle\} \quad (13)$$

which is the worst case infidelity for each trajectory  $\rho_{\sigma}(t)$ ,  $\sigma \in \Lambda$ .

The simulation results with the clock-control monotonic algorithm are summarised in figures 1 and 2. Figure 1 (left side) shows that, for  $T_f^{(0)} = 5$  the final time converges to some value that is close to 0.85. For  $T_f^{(0)} = 0.5$ , the final time seems to converge to the

---

<sup>5</sup>This unitary operation is equivalent to the Z-gate considering  $|0\rangle \approx |\alpha\rangle$  and  $|1\rangle \approx |-\alpha\rangle$ . In other words, in terms of the unitary operation we want to steer  $|e_1\rangle = |0\rangle$  to  $|f_1\rangle = |0\rangle$  and to steer  $|e_2\rangle = |1\rangle$  to  $|f_2\rangle = -|1\rangle$ .

same value, close to 0.85. For  $T_f^{(0)} = 0.85$ , the values of  $T_f$  along the steps of the algorithm remains always close to the initial value. Figure 1 (right side) shows that the final infidelity is improved a lot by the algorithm for  $T_f^{(0)} = 5$ , a little bit for  $T_f^{(0)} = 0.5$  and almost nothing for  $T_f^{(0)} = 0.85$  which seems to be very close to the “optimal” final time. It must be stressed that the infidelity for the (unperturbed) adiabatic control for  $T_f = 0.85$  (without running the algorithm) is 0.0696. After running 80 iterations of the algorithm with  $T_f^{(0)} = 0.85$ , the gate infidelity is 0.0669, a really small improvement with respect to the (unperturbed) adiabatic control conceived with the optimal final time. Thus the main interest in this example is to find the best value of  $T_f$ .

Figure 2 shows that, in all cases, the control pulses generated by the algorithm seems to converge to the same control pulses (the difference is almost indistinguishable in the (top) figure 2. Note that we have introduced a saturation of  $u$  between  $-0.8$  and  $+0.8$ , which is compatible with the algorithm. The algorithm produces a small improvement of the adiabatic control conceived with the optimal final time by augmenting the control effort close to the beginning and to the end of the interval  $[0, T_f]$ . From the findings in last figure, one may say that the more important here is to optimise the time of the gate. In this case the (unperturbed) adiabatic control is almost so efficient than the “optimal” control that is generated by our algorithm. The bottom of Figure 2 depicts the seeds in the three cases  $T_f^{(0)} = 5$ ,  $T_f^{(0)} = 0.5$  and  $T_f^{(0)} = 0.85$ . They are in fact the slightly perturbed adiabatic controls for each correspondent case.

One can run this algorithm for more complete models that includes for instance the “buffer” cavity, and then one may tune the final time of adiabatic control. This could be done even in the case that the quantum gate is generated by a series of different adiabatic control pulses

## 6.2 CNOT-gate

The notations similar to those of previous sub-section are used here. Following [8, equation (16)] where we have added single photon losses of rate  $\kappa_1$ , the master equation describing the evolution with scalar control input  $u(t)$  is given by

$$\begin{aligned} \frac{d\rho}{dt} = & -\mathbf{r}u[(a_{co} + a_{co}^\dagger - 2\alpha I_{co}) \otimes (a_{ta}^\dagger a_{ta} - \alpha^2 I_{ta}) \otimes I_{qu}, \rho] \\ & -\mathbf{r}g_2[(a_{co}^2 - \alpha^2) \otimes I_{ta} \otimes |e\rangle\langle g| + ((a_{co}^\dagger)^2 - \alpha^2) \otimes I_{ta} \otimes |g\rangle\langle e|, \rho] \\ & +k_2\mathcal{D}[(a_{co}^2 - \alpha^2 I_{co}) \otimes I_{ta} \otimes I_{qu}]\rho \\ & +k_1\mathcal{D}[a_{co} \otimes I_{ta} \otimes I_{qu}]\rho + k_1\mathcal{D}[I_{co} \otimes a_{ta} \otimes I_{qu}]\rho \end{aligned}$$

where  $\alpha^2 = 4$ ,  $k_2 = 1$ ,  $k_1 = \frac{1}{1000}$ ,  $g_2 = 10$  and  $k_2 T_f \approx 1$ . The underlying Hilbert-space is the tensor of three Hilbert-space  $\mathcal{H}_{co} \otimes \mathcal{H}_{ta} \otimes \mathcal{H}_{qu}$ : Hilbert-space of the control cat-qubit  $\mathcal{H}_{co}$ , Hilbert-space of the target cat-qubit  $\mathcal{H}_{ta}$ , Hilbert-space of an ancillary qubit  $\mathcal{H}_{qu} \equiv \mathbb{C}^2$ . The operators  $a_{co}$  and  $a_{ca}$  are the annihilation operators of the control and target cat-qubits. Denote by  $|\alpha/\alpha\rangle_{co/ta} \approx |0_L/1_L\rangle_{co/ta}$  the coherent states for the control and target cat-qubits, and by  $|g\rangle$  and  $|e\rangle$  the ground and excited states of the qubit. In the context of unitary transformations, the CNOT-gate is the operator that maps  $e_1 = |0_L\rangle_{co} \otimes |0_L\rangle_{ta} \otimes |g\rangle$  to  $f_1 = |0_L\rangle_{co} \otimes |0_L\rangle_{ta} \otimes |g\rangle$ ,  $e_2 = |0_L\rangle_{co} \otimes |1_L\rangle_{ta} \otimes |g\rangle$  to  $f_2 = |0_L\rangle_{co} \otimes |1_L\rangle_{ta} \otimes |g\rangle$ ,  $e_3 = |1_L\rangle_{co} \otimes |0_L\rangle_{ta} \otimes |g\rangle$  to  $f_3 = |1_L\rangle_{co} \otimes |1_L\rangle_{ta} \otimes |g\rangle$  and  $e_4 = |1_L\rangle_{co} \otimes |1_L\rangle_{ta} \otimes |g\rangle$  to  $f_4 = |1_L\rangle_{co} \otimes |0_L\rangle_{ta} \otimes |g\rangle$ . As

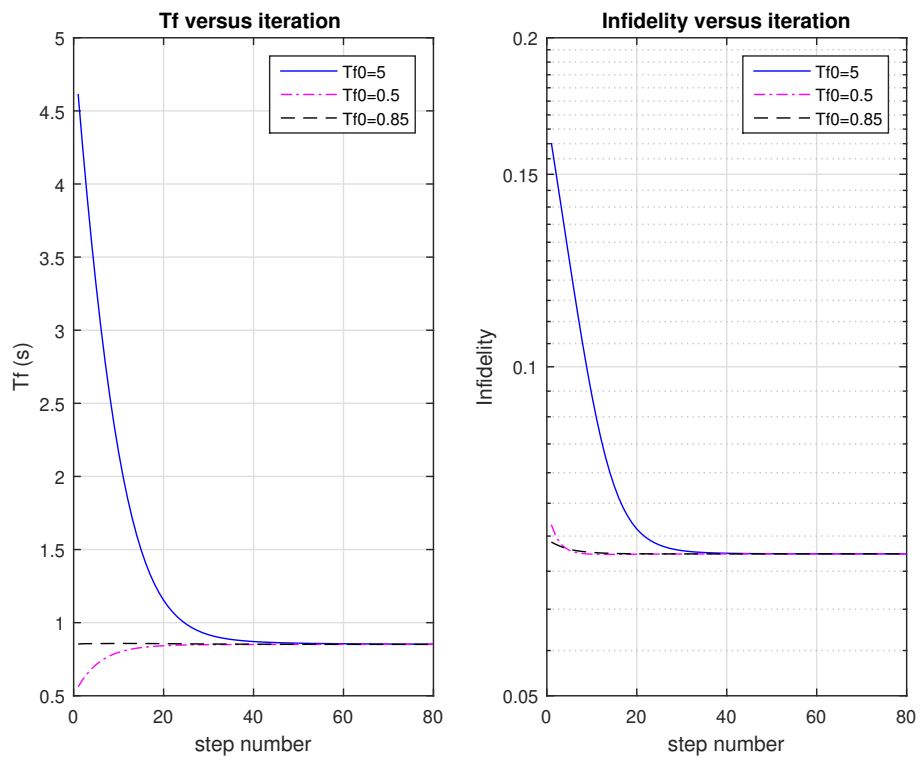


Figure 1: Z-gate generation. Left side: evolution of  $T_f$  and of infidelity  $\mathcal{I}$  (see (13)). In these simulations  $T_f^{(0)} = 5$ ,  $T_f^{(0)} = 0.85$ , and  $T_f^{(0)} = 0.5$  ( $\kappa_1 = 1/100$ ). Right side: infidelity that is obtained for each iteration of the algorithm for  $T_f^{(0)} = 0.85$ , and  $T_f^{(0)} = 0.5$ .

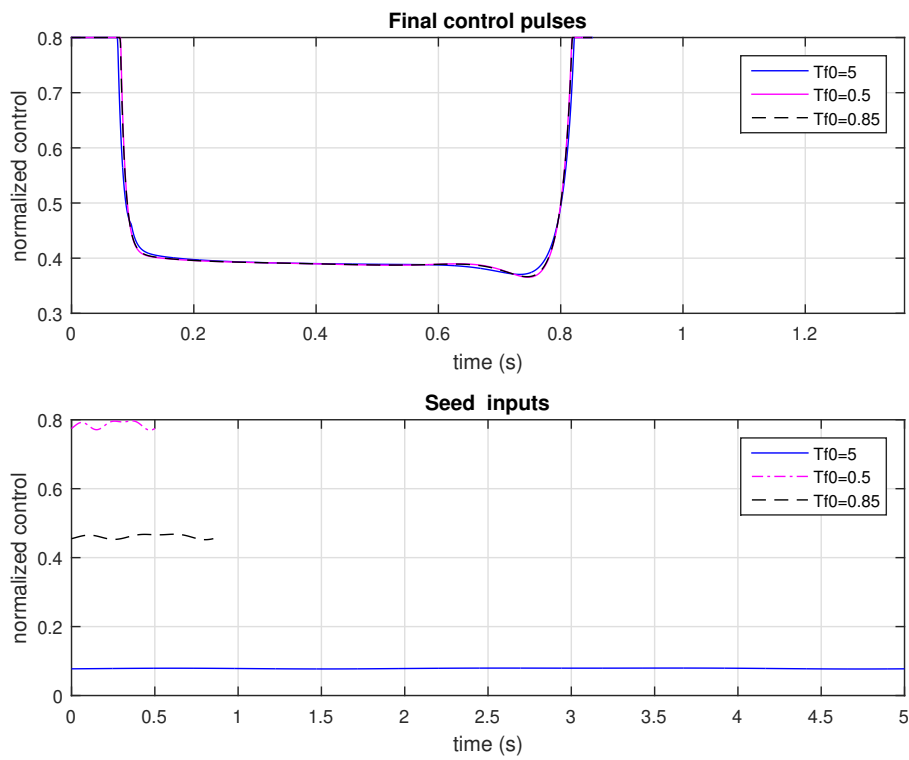


Figure 2: Z-gate generation. Top: Final control pulses for  $T_f^{(0)} = 5$ , for  $T_f^{(0)} = 0.85$ , and for  $T_f^{(0)} = 0.5$  ( $\kappa_1 = 1/100$ ). Bottom: The seed inputs for each case,  $T_f^{(0)} = 5$ , for  $T_f^{(0)} = 0.85$ , and for  $T_f^{(0)} = 0.5$  (seed inputs are slightly perturbed constant adiabatic control (11)).



in Definition 2, the operations that define the CNOT-gate in the context of density matrices are:

- (i) steer  $|e_i\rangle\langle e_i|$  to  $|f_i\rangle\langle f_i|$  at  $t = T_f$ , for  $i = 1, \dots, 4$ ;
- (ii) steer  $|e_{ijR}\rangle\langle e_{ijR}|$  to  $|f_{ijR}\rangle\langle f_{ijR}|$  at  $t = T_f$  and
- (iii) steer  $|e_{ijI}\rangle\langle e_{ijI}|$  to  $|f_{ijI}\rangle\langle f_{ijI}|$  at  $t = T_f$  for all  $i, j \in \{1, \dots, 4\}$  with  $i > j$ .

Simulations shows that<sup>6</sup> only the conditions (i) are sufficient to generate the gate up to a very good precision. The improvement of the infidelity of considering both conditions (i) and (ii) is less that 1% but the computation effort is four times greater. All the presented simulations considers only the conditions (i) for the construction of the Lyapunov function. The (in)fidelity that is presented considers only the set of conditions (i), but the complete set of conditions (i), (ii) and (iii) are considered for computing the final (in)fidelity, which we call by<sup>7</sup> “corrected-infidelity”. It well known that a nice (constant) adiabatic control for generating a CNOT gate at  $t = T_f$  is given by  $u = u_{ad} = \frac{\pi}{4\alpha T_f}$ .

The proof of Theorem 1 shows that the Lyapunov function of the end of Step  $\ell$  is equal to the Lyapunov function of the begining of step  $\ell + 1$ . However the numerical integration induces and error that is reflected by a difference of these values. This numerical difference can be used to estimate the numerical error of the Runge-Kutta integration. This can be used to find a convenient time-step of the integration. Also, the number of levels of both resonators for the truncated models were estimated to be at least  $n = 17$  for  $\alpha = 2$ . A greater value of  $\alpha$  will certainly need a greater  $n$  to in order to ensure the same precision. This means that the underlying Hilbert-space has dimension  $n \times n \times 2 = 578$ . So the  $578 \times 578$ -density matrix of the system represents a state of dimension 334084 for the Runge-Kutta integration of the ODE system For the next results we have considered a a slightly perturbed adiabatic control defined for  $T_f^{(0)} = 1.5$  as the seed of the algorithm with the same form (12) with  $T = T_f^{(0)}$ ,  $\mathbf{A} = \frac{2|u_{ad}|}{1000}$ ,  $M = 3$ .

At the top of Figure 3 the evolution of the infidelity  $\mathcal{I} = 1 - \mathcal{F}$  s presented along the steps of the algorithm. The final (uncorrected) infidelity 0.0009784 is attained in step 1249 of the algorithm. The final corrected<sup>8</sup> infidelity at the step 1249 is 0.0009865. The variation between the corrected and the uncorrected value is  $\approx 0.84\%$ . At the bottom of same figure, the evolution of the gate time  $T_f$  is presented. A final  $T_f = 1.259s$  is attained in step 1259 of the algorithm. At the top of Figure 3 it is presented the final control pulse that is constructed in step 1259. It can be compared with the constant adiabatic control for the same gate time  $T_f = 1.259s$  and the seed input of the algorithm. It is interesting to say that the definite integral of the final control pulse and the constant adiabatic control on  $[0, T_f]$  is respectively given and 3.92721 and 3.92699, corresponding to a variation of only 0.6%. However, the infidelity of the constant adiabatic pulse defined with the gate time  $T_f = 1.259s$  is 0.00143, which is more that 40% bigger that the one of our final control pulse that is produced by our algorithm. In some sense, our final control pulse is an optimised adiabatic control, since the integral is almost conserved. The bottom of figure 4 shows the final fidelity of the constant adiabatic control as a function of the gate time  $T_f$ . The optimal value of the infidelity of the constant adiabatic control shown in Figure 4 is close to 0.00128 (corresponding to  $T_f \approx 1.8s$ ),

<sup>6</sup>This property that ensures that conditions (ii) and (iii) are not important is due to particular symmetries if the system. See also [10] for interesting and connected results.

<sup>7</sup>The infidelity correction when one computes the worst case of all the conditions (i), (ii), (ii) with respect to the infidelity computed only with the set of conditions (i) is approximately given by 0,8% in all cases.

<sup>8</sup>Corrected in the sense that it considers the worst case infidelity of all the 16 conditions (i) and (ii) of definition 2.

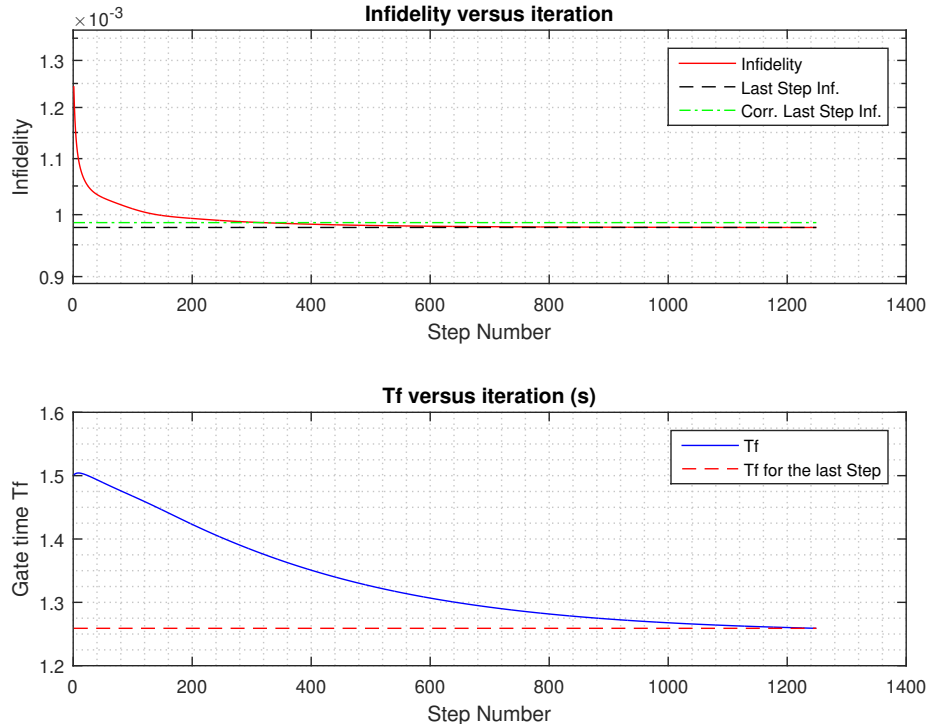


Figure 3: CNOT-gate. Top: Evolution of gate-infidelity along the steps of the algorithm. The (uncorrected) infidelity (see (13)) of the last step is given by  $0.9784 \times 10^{-3}$ . The corrected infidelity of the last step is  $0.98655 \times 10^{-3}$  (the variation between the corrected and the uncorrected value is  $\approx 0.84\%$ ). Bottom: The evolution of the gate-time  $T_f$  along the steps of the algorithm. The gate-time for the last step is  $T_f = 1.259$ .

which is 29.2% greater than (corrected) infidelity of the final “optimal” control pulse. Anyway, it is clear that the pulse shape is rather important in this second example. For the second example, the problem of optimising the fidelity with respect to the gate-time of a constant adiabatic control (which concerns to plot of the bottom of Figure 4) gives a rather different final infidelity when one optimises both the gate-time and the shape of the control input, which concerns to the result of our algorithm depicted in Figure 3.

## 7 Conclusions

A monotonic numerical method for generating quantum gates for open systems is described in this work. This method is strongly related to a *Smooth-Case* version of the Krotov method that considers *sequential* input update, that is, the input is updated “on the fly” of the simulation of the system dynamics [13, 10]. Our algorithm is generalised in this work by including the so-called *clock-control*, which was shown to be equivalent to an algorithm that converges to the stationary conditions of an optimal control problem that regards not only the shape of the control pulses, but also seeks an optimal gate-time  $T_f$ . The effectiveness of this generalised algorithm was tested in two case-studies of physical interest (confined cat-qubit gates), showing promising results and the ability of obtaining the optimal gate-time and optimal control pulses for these two examples. The standard form of such algorithm called

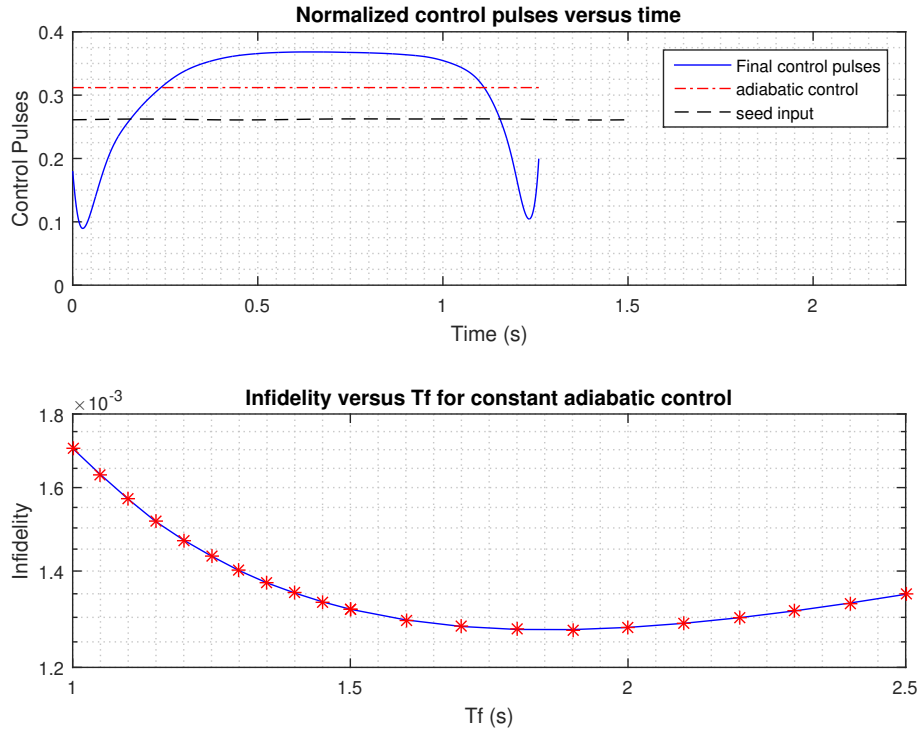


Figure 4: CNOT-gate. Top: Final control pulses generated by the algorithm of section ref-sClock. The constant adiabatic control for the same  $T_f$  of the final control pulses is also presented along with the seed of the algorithm, which is a slightly perturbed adiabatic control defined for a initial gate-time  $T_f^{(0)} = 1.5s$ . Bottom: Infidelity that was obtained after simulating a constant adiabatic control presented as a function of gate-time  $T_f$ . The minimum infidelity is close to 0.00128 for  $T_f = 1.8$ , whereas the infidelity obtained with algorithm is 0.00098655 with a shorter optimized time  $T_f = 1.259$ .

RIGA in [24] is different from the algorithm that is presented in this work. In [4], the authors shows how one obtains, for Hamiltonian dynamics the presented algorithm from RIGA . It is also shown in [4] that GRAPE is a kind of discrete version of RIGA when the objective function is the Lyapunov function, and when there is no sequential update, that is, the input is updated only in the end of each step of the algorithm.

## References

- [1] K. Beauchard, P. S. Pereira da Silva, and Pierre Rouchon. Stabilization for an ensemble of half-spin systems. *Automatica*, 48(1):68–76, 2012.
- [2] H.P. Breuer and F. Petruccione. *The Theory of Open Quantum Systems*. Oxford University Press, 2002.
- [3] J.-M. Coron. *Control and Nonlinearity*. American Mathematical Society, 2007.
- [4] P. S. Pereira da Silva and P. Rouchon. On numerical methods for generating quantum gates. In *in preparation*, 2024.
- [5] P. de Fouquieres, S.G. Schirmer, S.J. Glaser, and Ilya Kuprov. Second order gradient ascent pulse engineering. *Journal of Magnetic Resonance*, 212(2):412 – 417, 2011.
- [6] D. Dong and I. R. Petersen. Quantum control theory and applications: a survey. *IET Control Theory Applications*, 4(12):2651–2671, December 2010.
- [7] M. Fliess, J. Levine, P. Martin, F. Ollivier, and P. Rouchon. Controlling nonlinear systems by flatness. In Christopher I. Byrnes, Biswa N. Datta, Clyde F. Martin, and David S. Gilliam, editors, *Systems and Control in the Twenty-First Century*, pages 137–154, Boston, MA, 1997. Birkhäuser Boston.
- [8] R. Gautier, A. Sarlette, and M. Mirrahimi. Combined dissipative and hamiltonian confinement of cat qubits. *PRX Quantum*, 3:020339, May 2022.
- [9] S.J. Glaser, U. Boscain, T. Calarco, C.P. Koch, W. Köckenberger, R. Kosloff, I. Kuprov, B. Luy, S. Schirmer, T. Schulte-Herbrüggen, D. Sugny, and F.K. Wilhelm. Training Schrödinger’s cat: quantum optimal control. *Eur. Phys. J. D*, 69(12), December 2015.
- [10] Michael H Goerz, Daniel M Reich, and Christiane P Koch. Optimal control theory for a unitary operation under dissipative evolution. *New Journal of Physics*, 16(5):055012, may 2014.
- [11] Symeon Grivopoulos and Bassam Bamieh. Lyapunov-based control of quantum systems. In *Decision and Control, 2003. Proceedings. 42nd IEEE Conference on*, volume 1, pages 434–438. IEEE, 2003.
- [12] N. Khaneja, T. Reiss, C. Kehlet, T. Schulte-Herbrüggen, and S. J. Glaser. Optimal control of coupled spin dynamics: design of nmr pulse sequences by gradient ascent algorithms. *Journal of Magnetic Resonance*, 172(2):296 – 305, 2005. DOI: 10.1016/j.jmr.2004.11.004.

- [13] Christiane P Koch. Controlling open quantum systems: tools, achievements, and limitations. *Journal of Physics: Condensed Matter*, 28(21):213001, may 2016.
- [14] Shai Machnes, Elie Assémat, David Tannor, and Frank K. Wilhelm. Tunable, flexible, and efficient optimization of control pulses for practical qubits. *Phys. Rev. Lett.*, 120:150401, Apr 2018.
- [15] U. A. Maciel Neto, P. S. Pereira da Silva, and P. Rouchon. Motion planing for an ensemble of bloch equations towards the south pole with smooth bounded control. *Automatica*, 145:110529, 2022.
- [16] Mazyar Mirrahimi. Lyapunov control of a quantum particle in a decaying potential. In *Annales de l'Institut Henri Poincaré (C) Non Linear Analysis*, volume 26, pages 1743–1765. Elsevier, 2009.
- [17] Mazyar Mirrahimi, Zaki Leghtas, Victor V Albert, Steven Touzard, Robert J Schoelkopf, Liang Jiang, and Michel H Devoret. Dynamically protected cat-qubits: a new paradigm for universal quantum computation. *New Journal of Physics*, 16(4):045014, 2014.
- [18] Mazyar Mirrahimi, Pierre Rouchon, and Gabriel Turinici. Lyapunov control of bilinear schrödinger equations. *Automatica*, 41(11):1987–1994, 2005.
- [19] Michael A. Nielsen and Isaac L. Chuang. *Quantum Computation and Quantum Information: 10th Anniversary Edition*. Cambridge University Press, USA, 10th edition, 2011.
- [20] José P. Palao and Ronnie Kosloff. Quantum computing by an optimal control algorithm for unitary transformations. *Phys. Rev. Lett.*, 89(18):188301–, October 2002.
- [21] José P. Palao and Ronnie Kosloff. Optimal control theory for unitary transformations. *Phys. Rev. A*, 68(6):062308–, December 2003.
- [22] Yu Pan, V. Ugrinovskii, and M. R. James. Lyapunov analysis for coherent control of quantum systems by dissipation. In *2015 American Control Conference (ACC)*, pages 98–103, July 2015.
- [23] P. S. Pereira da Silva and P. Rouchon. RIGA and FPA, quantum control with smooth control pulses [source code]. *CODE OCEAN*, 2019. <https://doi.org/10.24433/CO.3293651.v2>.
- [24] Paulo S. Pereira da Silva, H. Bessa Silveira, and P. Rouchon. Fast and virtually exact quantum gate generation in  $u(n)$  via iterative lyapunov methods. *International Journal of Control*, 0(0):1–15, 2019.
- [25] N. Rach, M. M. Müller, T. Calarco, and S. Montangero. Dressing the chopped-random-basis optimization: A bandwidth-limited access to the trap-free landscape. *Phys. Rev. A*, 92:062343, Dec 2015.
- [26] S G Schirmer and Pierre de Fouquieres. Efficient algorithms for optimal control of quantum dynamics: the krotov method unencumbered. *New Journal of Physics*, 13(7):073029–, 2011.

- [27] R. Sepulchre, A. Sarlette, and P. Rouchon. Consensus in non-commutative spaces. In *Decision and Control (CDC), 2010 49th IEEE Conference on*, pages 6596–6601, 2010.
- [28] H. B. Silveira, P. S. Pereira da Silva, and P. Rouchon. Quantum gate generation by T-sampling stabilization. *International Journal of Control*, 87(6):1227–1242, 2014.
- [29] H. B. Silveira, P. S. Pereira da Silva, and P. Rouchon. Quantum gate generation for systems with drift in  $u(n)$  using Lyapunov-Lasalle techniques. *International Journal of Control*, 89(1):1–16, 2016. DOI:10.1080/00207179.2016.1161830.
- [30] Naoki Yamamoto, Koji Tsumura, and Shinji Hara. Feedback control of quantum entanglement in a two-spin system. *Automatica*, 43(6):981 – 992, 2007.
- [31] Jing Zhang, Yu-xi Liu, Re-Bing Wu, Kurt Jacobs, and Franco Nori. Quantum feedback: theory, experiments, and applications. *arXiv preprint arXiv:1407.8536*, 2014.

## A Numerical implementation

The numerical integration of the systems and their adjoints considers the equations of Section 4. All this is implemented as matrix version of 4th-order Runge-Kutta (fixed step) method, which regards sums and multiplications of  $n \times n$  matrices. We have implemented this in a MATLAB program, but it is clear that a GPU implementation could improve a lot the run-time of the method. As described in Section 4, all the backwards integrated paths of the adjoint system  $J_\sigma(t_k), \sigma \in \Lambda$  for the discrete time  $t_k = \frac{kT_f}{N_{sim}}, k = 0, \dots, N_{sim}$  must be saved in memory. For instance, in the simulation of the second example, we have chosen  $N_{sim} = 1000$ , where  $N_{sim}$  is the number of Runge-Kutta steps, in order to ensure a good precision<sup>9</sup>. For large dimensional systems, one may have a memory overflow. In order to avoid this, one could do the backwards integration of step #2 of the algorithm without saving all the data in memory, but only saving the “final conditions”  $J_\sigma(0), \sigma \in \Lambda$ , and then perform a forward integration using that data as initial conditions. The numerical stability is ensured for the adjoint system for the backwards integration because such system coincides with the Heisenberg point of view, and hence is stable (from a dynamic system perspective). However the forward integration of the adjoint system (which may be unstable from a dynamic system point of view) may present bad numerical properties in some examples. In order to overcome this, one may save for instance, the backwards integrated data  $J_\sigma(t_k)$  for  $k = 0, 10, 100, \dots$  and do the forward integration by resetting the initial conditions to these values for  $t_k, k = 0, 10, 100, \dots$ . This will divide the memory space by a factor of 10 and will preserve the numerical precision as well.

As a last remark, it is important to say that one may include input limitations in the algorithm. When there is no clock-control, one may do this by standard saturation of the control-law by its maximal value. It is clear that the seed input must also obey this restriction. When the clock-control is present, one may saturate the clock control  $\bar{v}_0(t)$  in a standard way, but since the other controls  $\bar{v}_k(t), k > 0$  are virtual controls, the saturation of these controls must be corrected by the factor  $1 + v_0(t)$  that multiplies the real controls in order to compute the virtual controls. This is done in a way that the contribution of each virtual

---

<sup>9</sup>As said in Example 2, the numerical precision may be estimated by the numerical difference of the Lyapunov function of the end of step  $\ell$  and the one of the of step  $\ell + 1$  which in theory must be exactly the same. The difference that is obtained is then caused by the error of the numerical integration.

feedback  $\tilde{v}_k(t), k = 0, 1, \dots, m$  to the derivative of the Lyapunov function is always non-positive. Consider the saturation map:

$$\text{sat}(x, A, -B) = \begin{cases} x, & \text{if } x \in [-B, A] \\ -B, & \text{if } x < -B \\ A, & \text{if } x > A \end{cases} \quad (14)$$

The saturated feedback that was used in the simulations of this work is of the form:

$$\tilde{v}_k(t) = \text{sat}(g_k F_k, A_k, -B_k), k = 0, 1, \dots, m \quad (15)$$

where  $\tilde{v}_k(t) = g_k F_k$  is the standard “non-saturated” feedback law, and

$$F_k = \sum_{\sigma \in \Lambda} \text{trace}(J_\sigma(\tau) \mathcal{L}_k(\rho_\sigma(\tau))), k = 0, 1, \dots, m.$$

Furthermore,  $A_0 = u_{max}^0$ ,  $-B_0 = \max\{-u_{max}^0, -\frac{\bar{u}^{\ell-1}}{u_k^{max}} - 1, \frac{\bar{u}^{\ell-1}}{u_k^{max}} - 1, k = 1, \dots, m\}$ , and  $A_k = B_k = (1 + v_0)u_0^{max}, k = 1, \dots, m$ .

This saturated control has a theoretical explanation given in the sequel. Recall that the the control law is of the form (see Section 5) :

$$\bar{v}_k^\ell(\tau) = \bar{u}^{\ell-1}(\tau) + \tilde{v}_k(\tau), k = 1, \dots, m$$

It is easy to see that the derivative of the Lyapunov function is

$$\frac{d}{d\tau} \mathcal{V} = - \sum_{k=0}^m \tilde{v}_k(t) F_k(t)$$

Then the following result holds:

**Proposition: 2** *Assume that  $|\bar{u}^{\ell-1}| \leq u_k^{max}$  for  $u_k^{max} > 0, k = 0, \dots, m$ . Consider a control law of the form (15) such that  $\tilde{v}_k(t) F_k \geq 0$ , in any circumstances<sup>10</sup> and  $|\bar{u}^{\ell-1}| \leq u_k^{max}, k = 0, \dots, m$ . Suppose that a given  $\tilde{v}_0$  maximises the product  $\tilde{v}_0(\tau) F_0(\tau)$ . Assume that the other virtual feedback  $\tilde{v}_k(\tau), k = 1, \dots, m$  minimizes  $\frac{d\mathcal{V}}{d\tau}$  for this given  $v_0$ . Then  $A_0 = u_{max}^0$ ,  $B_0 = -\max\{-u_{max}^0, -\frac{\bar{u}^{\ell-1}}{u_k^{max}} - 1, \frac{\bar{u}^{\ell-1}}{u_k^{max}} - 1, k = 1, \dots, m\}$ ,  $A_k = (1 + v_0)u_k^{max} - \bar{u}^{\ell-1}$ , and  $B_k = (1 + v_0)u_k^{max} + \bar{u}^{\ell-1}, k = 1, \dots, m$ .*

**Proof:** Since  $\tilde{v}_k(\tau) F_k(\tau) \geq 0$  for all  $k = 0, \dots, m$  in all circumstances without knowing the signal of  $F_k(\tau)$  *a priori*, this means that the intervals  $[-B_k, A_k]$  must contain zero, otherwise we cannot choose freely the signal of  $\tilde{v}_k(\tau) F_k(\tau)$  when the algorithm is running. As  $\bar{u}^\ell = \frac{\bar{u}^{\ell-1}(\tau) + \tilde{v}_k(\tau)}{1 + v_0}$ , and  $\bar{u}^\ell \leq u_k^{max}$  this means that  $\tilde{v}_k \leq (1 + v_0)u_k^{max} - \bar{u}^{\ell-1} = A_k \geq 0$  and  $\tilde{v}_k \geq -(1 + v_0)u_k^{max} - \bar{u}^{\ell-1} = -B_k \leq 0$ . This implies that  $v_0 \geq \frac{\bar{u}^{\ell-1}}{u_k^{max}} - 1$  and  $v_0 \geq \frac{\bar{u}^{\ell-1}}{u_k^{max}} - 1$ . The rest of the statement is straightforward and is left to the reader.  $\square$

<sup>10</sup>The signal of  $F_k(\tau)$  is not known a priori.